International Journal of Cardiology 316 (2020) 130–136

Contents lists available at ScienceDirect

International Journal of Cardiology

journal homepage: www.elsevier.com/locate/ijcard

A morphology based deep learning model for atrial fibrillation detection using single cycle electrocardiographic samples

Sarah W.E. Baalman [a,1], Florian E. Schroevers [b,1], Abel J. Oakley [b,1], Tom F. Brouwer [a,1], Willeke van der Stuijt [a,1], Hidde Bleijendaal [a,1], Lucas A. Ramos [a,1], Ricardo R. Lopes [a,1], Henk A. Marquering [a,1], Reinoud E. Knops [a,1], Joris R. de Groot [a,*,1]

[a] Amsterdam UMC, University of Amsterdam, Heart Center, Department of Clinical and Experimental Cardiology, Amsterdam Cardiovascular Sciences, Meibergdreef 9, Amsterdam, the Netherlands
[b] Amsterdam University of Amsterdam, Faculty of Science, Science Park 904, Amsterdam, the Netherlands

ARTICLE INFO

Article history:
Received 10 March 2020
Received in revised form 3 April 2020
Accepted 16 April 2020
Available online 18 April 2020

Keywords:
Deep learning
Atrial fibrillation
Electrocardiogram
Morphology
Black box
Visualization

ABSTRACT

Background: Deep learning (DL) has shown promising results in improving atrial fibrillation (AF) detection algorithms. However, these models are often criticized because of their "black box" nature.
Aim: To develop a morphology based DL model to discriminate AF from sinus rhythm (SR), and to visualize which parts of the ECG are used by the model to derive to the right classification.
Methods: We pre-processed raw data of 1469 ECGs in AF or SR, of patients with a history AF. Input data was generated by normalizing all single cycles (SC) of one ECG lead to SC-ECG samples by 1) centralizing the R wave or 2) scaling from R-to- R wave. Different DL models were trained by splitting the data in a training, validation and test set. By using a DL based heat mapping technique we visualized those areas of the ECG used by the classifier to come to the correct classification.
Results: The DL model with the best performance was a feedforward neural network trained by SC-ECG samples on a R-to-R wave basis of lead II, resulting in an accuracy of 0.96 and F1-score of 0.94. The onset of the QRS complex proved to be the most relevant area for the model to discriminate AF from SR.
Conclusion: The morphology based DL model developed in this study was able to discriminate AF from SR with a very high accuracy. DL model visualization may help clinicians gain insights into which (unrecognized) ECG features are most sensitive to discriminate AF from SR.

1. Introduction

Atrial fibrillation (AF) is the most common cardiac arrhythmia worldwide and associated with a five-fold increased risk of ischemic stroke and a doubled mortality rate [1]. Standard of care for AF detection is human confirmation of AF documented on an electrocardiogram (ECG), device (i.e. pacemaker, implantable defibrillators or implantable loop recorder) acquired atrial electrogram (EGM) or Holter recording. ECGs of patients in AF are characterized by the absence of P-waves and irregular R-R intervals. Most automated non-deep learning algorithms integrated in ECG machines and cardiac devices rely on these two characteristics. However, misdiagnosis of AF by these classic algorithms remains common as noise and baseline wander may affect detection of the P-wave, and R-R interval based algorithms require prolonged recordings to identify AF [2,3].

Deep learning (DL) has shown to improve current AF detection and classification algorithms remarkably [4–6]. DL is a subfield of artificial intelligence (AI) and often consists of neural networks with multiple deep layers that are capable of learning representations of data with multiple levels of abstraction [7]. The capability of DL models to recognize and discriminate specific patterns by learning features from raw input data, makes DL a promising and interesting training tool for ECG interpretation and rhythm detection and discrimination models [6]. Especially, as DL carries the possibility to use ECG samples with a short duration and thereby only focuses on morphology instead of R-R interval with a similar high accuracy [8,9]. Thereby, human interpretation can potentially be improved through understanding which segments of the ECG are most relevant for the discrimination of AF from SR. Despite the reported high diagnostic performances of previous DL-based AF detection models, these models are often criticized because it is unclear

* Corresponding author at: Amsterdam UMC, University of Amsterdam, Heart Center, Department of Clinical and Experimental Cardiology, Cardiovascular Sciences, PO Box 22700, Meibergdreef 9, 1105 AZ, Amsterdam, the Nertherlands.
E-mail address: j.r.degroot@amsterdamumc.nl (J.R. de Groot).
[1]This author takes responsibility for all aspects of the reliability and freedom from bias of the data presented and their discussed interpretation.

https://doi.org/10.1016/j.ijcard.2020.04.046

how these models derive their classification decision: the "black box" criticism [10].

The aim of our study is therefore to develop and test a morphology based DL model to discriminate AF from SR based on single cycle ECG (SC-ECG) samples of ECGs performed in our tertiary referral center, and to visualize which part of the SC-ECG samples is used by the model to come to a classification decision.

2. Methods

2.1. Data source and adjudication

We developed a DL model to discriminate AF from SR from pre-processed raw signals of 12-lead ECGs sampled at 500 Hz for a duration of 10 s of patients diagnosed with paroxysmal or persistent AF. The dataset consisted of 1499 ECGs of patients participating in the Atrial Fibrillation Ablation and Autonomic Modulation via Thoracoscopic Surgery (AFACT) trial that investigated epicardial ganglion plexus ablation during thoracoscopic PVI for advanced AF [11]. Of all patients electrocardiographic documentation of AF was available. ECGs were obtained in all patients before surgery and every three months during one year follow up. All 12-lead ECGs were adjudicated by two experienced investigators as SR, AF or other arrhythmias. In case of disagreement a third adjudicator was asked to determine the rhythm. Only ECGs adjudicated as AF or SR, regardless of noise or ectopic beats, were included in the dataset. ECGs of any other supraventricular tachycardia (SVT) (e.g. atrial flutter or atrial tachycardia) were excluded for the development of the model.

2.2. Pre-processing

Fig. 1 shows an overview of pre-processing of the raw ECG signals to SC-ECG samples, to train, validate and test different DL models. Raw ECG signals of eight different channels (I, II, V1–V6) were pre-processed with several open source algorithms. First, the data was smoothed with the Savitzky-Golay filter, which uses convolutions and local polynomial fitting to smooth the 500 Hz ECG signals [12]. To correct for baseline wander we used the Fourier Cosine Series to strengthen the baseline to zero [13]. To simplify the learning process we only used data from one ECG lead (lead II) for the development of our first DL models to discriminate AF from SR.

2.2.1. Single cycle ECG samples

SC-ECG samples suitable for DL processing were created automatically by standardizing all single cardiac cycles of one ECG lead in an identical way in both space and time. Accordingly, all SC-ECG samples were normalized to an identical number of data points in two different ways (Fig. 1): *Experiment 1* - by centralizing the R wave, allowing an equal number of data points before and after the QRS complex, and the same resolution across different ECGs; *Experiment 2* - by normalizing each cardiac cycle from R-to-R wave, allowing inclusion of the entire cardiac cycle in the analysis, but with different resolution across ECGs. The Hamilton segmenter algorithm was used to locate the R waves on the ECG signals [14]. This led to a total amount of $Z(X) = 1469X$ samples, wherein X is the number of cardiac cycles during 10 s of one lead (Fig. 1A, supplementary). Using all single cardiac cycles from lead II, this resulted in 15,744 and 15,735 SC-ECG samples for R-centered (*experiment 1*) or R-to-R representation (*experiment 2*) of the data respectively. The number of data points were reduced from 5000 (500 Hz × 10 s) to 80 data points per SC-ECG sample, using linear interpolation to adjust for a cardiac cycle with a shorter R-R interval without losing essential features.

2.3. Development of the different DL models

Multiple DL models with different layers and architectures were developed and trained by distributing the data equally such that 50% of the SC-ECG samples were SR and 50% AF. Subsequently, the data was split in a training (60%), validation (25%) and test (15%) set. The first DL model used the SC-ECG samples with a centered R-wave representation (*experiment 1*) of lead II as data input. The second model used SC-ECG samples with an R-to-R-wave representation (*experiment 2*) of lead II as input. We repeated training of the model with the best performance with data of the other seven leads (I, V1–V6) separately. Model performance was reported as accuracy and cross-entropy loss. The best performing model, hereafter the gold standard, was defined as the model with the highest accuracy, area under the ROC curve (ROC-AUC) and area under the precision recall curve (PR-AUC). Results of all best performing models of each lead were reported as accuracy, ROC-AUC, PR-AUC and F1-score [15]. Analysis was computed with Python, version 3.6.5 (Python Software Foundation).

2.4. Visualization

To visualize the segments of the ECG that were most relevant for AF detection in our best performing model, we developed a method to demonstrate which specific ECG features are used by the DL model to discriminate AF from SR. By adjusting the attention mechanism to a recurrent neural networks (RNN) to an attention mechanism to a feedforward neural network [16]. This feedforward model uses one hidden layer to maintain spatial distribution, by using a combination of weights of relevant data points to come to a correct classification. Visualization was represented by heat mapping the values of the attention vector on the input (e.g. flat input, or mean morphology of all SC-ECG samples in SR or AF).

2.5. Reproducibility & open science

Detailed information about the architecture and algorithms, including all python codes of our pre-processing, best performing model and visualization techniques will be made publicly available through GitHub [17]. All ECGs and patient data used for the development of our models will not become publicly available according to the General Data Protection Regulation (GDPR) within the European Union [18].

3. Results

The mean age of this patient population was 59.0 ± 8.2 years and 175 (73%) were male [11]. After adjudication, a total of 1469 (98%) out of the 1499 ECGs, consisting of 1058 (72%) ECGs with SR and 411 (28%) with AF, were included. Baseline ECG characteristics are shown in Table 1A (supplementary). Excluded ECGs (2%) only consisted of ECGs with SVT other than AF. Optimal scaling of all single cardiac cycles led to 80 data points for each SC-ECG sample. In addition, all SC-ECG samples were normalized in amplitude (divided by the maximum value), resulting in a range of each sample between −1 and 1. Fig. 2 shows the mean of the data points of all scaled SC-ECG samples classified as SR or AF, normalized following the two different representations of the data: R-centered (*experiment 1*) vs. R-to-R wave (*experiment 2*).

3.1. Best performing model

The architecture of the best performing model was a feedforward neural network consisting of seven hidden layers with rectified linear unit (ReLU) activation (first three dense layers) and linear activation (last four dense layers) (Fig. 2A, supplementary). The sigmoid function was used as activation function of the output node. Fig. 2B

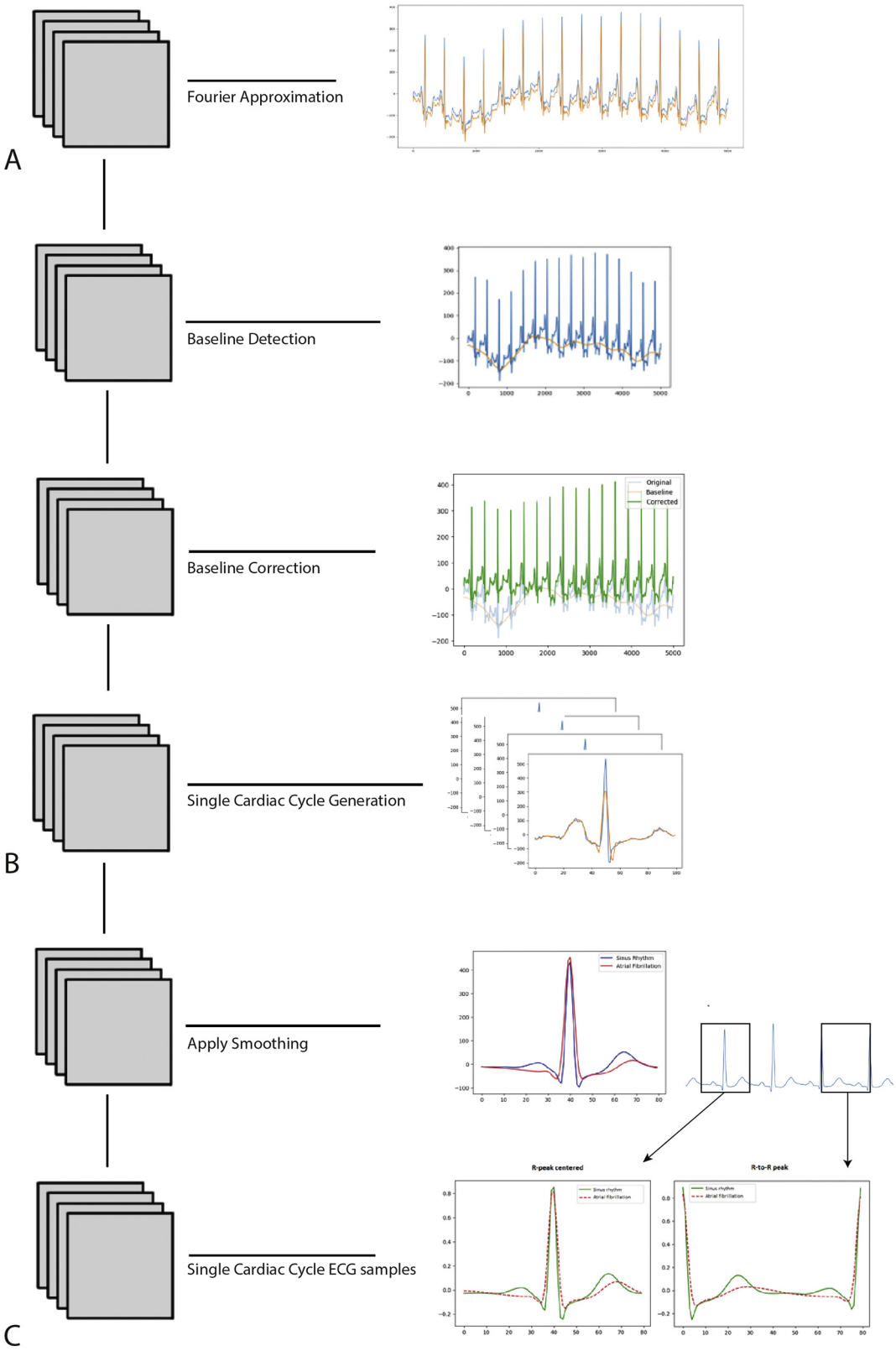

Fig. 1. Overview of pre-processing the raw 12-lead ECG signals to correct input data. A) The data was smoothed with the Savitzky-Golay algorithm. To correct for baseline wander we used the Fourier Cosine Series. B) SC-ECG samples were created by normalizing all single cardiac cycles of one ECG lead, of a 12-lead ECG sampled at 10 s in AF or SR, to an identical number of data points. C) SC-ECG samples were created in two different ways: by centralizing the R wave (left), and on a R-to-R wave driven way (right).

(supplementary) shows the accuracy and cross-entropy loss of the best performing model trained on R-centered (*experiment 1*) or R-to-R wave SC-ECG samples (*experiment 2*).

3.1.1. Experiment 1

Training the model with R-centered SC-ECG samples was done in 128 epochs (Fig. 2B, supplementary), of which the starting weight of

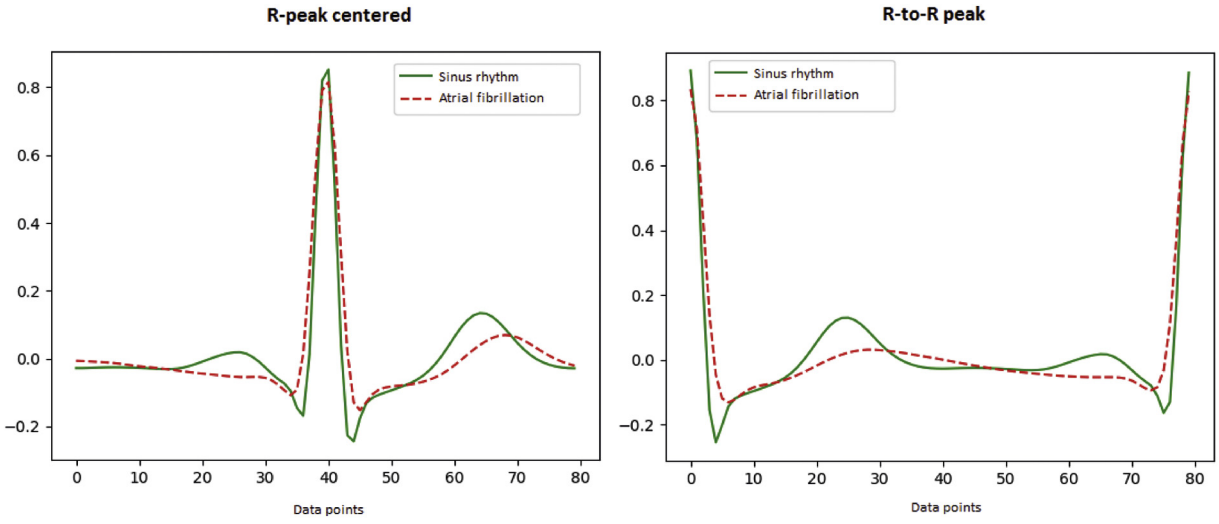

Fig. 2. Morphology of SC-ECG samples in AF or SR. Mean morphology of all SC-ECG samples in AF (dotted red line) and SR (solid green line) of both representations of the data. Experiment 1: R-wave centered SC-ECG samples (left). Experiment 2: R-to-R wave SC-ECG samples (right).

the net were determined by the last epoch, with the first epoch starting with Xavier uniformly distributed random weights. The model was optimized by using the Adam optimization algorithm to minimize the cross-entropy [19]. Dropout was used for regularization and to prevent overfitting (Fig. 2A, supplementary). This resulted in an ROC-AUC of 0.96, PR-AUC of 0.96 and accuracy of 0.94 (Table 1).

3.1.2. Experiment 2

Training the model with the 15,735 R-to-R wave SC-ECG samples was performed in 128 epochs (Fig. 2B, supplementary), resulting in an accuracy of 0.96, ROC-AUC of 0.97 and PR-AUC of 0.96 (Table 1). Table 1 shows the performance of the model after training with the R-to-R-wave SC-ECG samples of the other leads separately. The predictions of the signals from lead II and V3 (accuracy 0.96, ROC-AUC 0.97, PR-AUC 0.96) resulted in the best performances.

3.2. Deep learning model visualization

Fig. 3 shows heat mapping of the features of the ECG used by the DL model, trained on R-to-R wave SC-ECG samples (*experiment 2*) of lead II, for the classification predictions. The R-to-R wave representation (*experiment 2*) was chosen, because this representation had a numerically better performance and was expected to be affected by heart rate to a lesser extent and consequent deformation of the P and T wave. As shown in Fig. 3 the segments of the ECG that are most relevant for AF detection in the DL model with the best performance include the presence of the P-wave, the onset of the QRS complex and early and late components of the T-wave. The onset of the QRS complex was the most relevant time-window for the model to discriminate AF from SR. The results of our visualization technique were similar in the other 7 leads (*experiment 2*) that were not assessed by the network during training previously.

Table 1
Accuracy, PR-AUC, ROC-AUC and F1-score of different models trained with R-centered SC-ECG samples of lead II or R-to-R wave SC-ECG samples of different leads. Lead II and V3 resulted in the model with the best overall performance to discriminate SR from AF.

Input data	Lead	Accuracy	ROC-AUC	PR-AUC	F1-score
R-centered SC-ECG samples	II	0.94	0.96	0.96	0.81
R-to-R-wave SC-ECG samples	I	0.93	0.95	0.93	0.90
	II	0.96	0.97	0.96	0.94
	V1	0.95	0.98	0.96	0.93
	V2	0.94	0.96	0.95	0.91
	V3	0.96	0.97	0.96	0.94
	V4	0.95	0.97	0.95	0.93
	V5	0.95	0.97	0.96	0.92
	V6	0.94	0.96	0.93	0.91

SC-ECG, single cycle-ECG; ROC-AUC, area under the receiver operating curve; PR-AUC, area under the precision recall curve.

4. Discussion

We demonstrate that a good performing DL classification model can be developed using only the morphology of single cardiac cycles of one ECG lead. Second, our developed DL visualization tool demonstrated which specific ECG segments used by the DL algorithm best discriminated AF from SR.

4.1. Model performance

Our approach of using SC-ECG morphology instead of full time series is unique to classic rule based algorithms in that it discriminates AF from SR on a beat-to-beat morphology basis, rather than on a combination of morphology and time. Different representations of the raw ECG signals (R-centered vs. R-to-R wave) did not show any significant difference in performance. However, using data from different leads of the ECGs did affect the performance of the model (Table 1). The accuracy of more than 93% in all our models exceeds the reported accuracy of 71% in the commercially available algorithms integrated in current ECG machines [2]. Exclusion of ECGs in SVT other than AF (e.g. atrial flutter or atrial tachycardia) may have contributed to this improvement. However, we cannot exclude that our method of pre-processing the data on an R-centered basis, where the R wave is centered and the rest of complex is scaled to the predefined 80 data points, had an effect on the results due to the R-R irregularity in AF, as the absolute resolution of this approach was similar across ECGs but different when scaled to heart rate. Theoretically, this should have less of an effect on the R-to-R complex representation as simply all the data points between two R waves were taken and scaled to an 80 data points dimension, with implications on different resolutions across different single cardiac cycles.

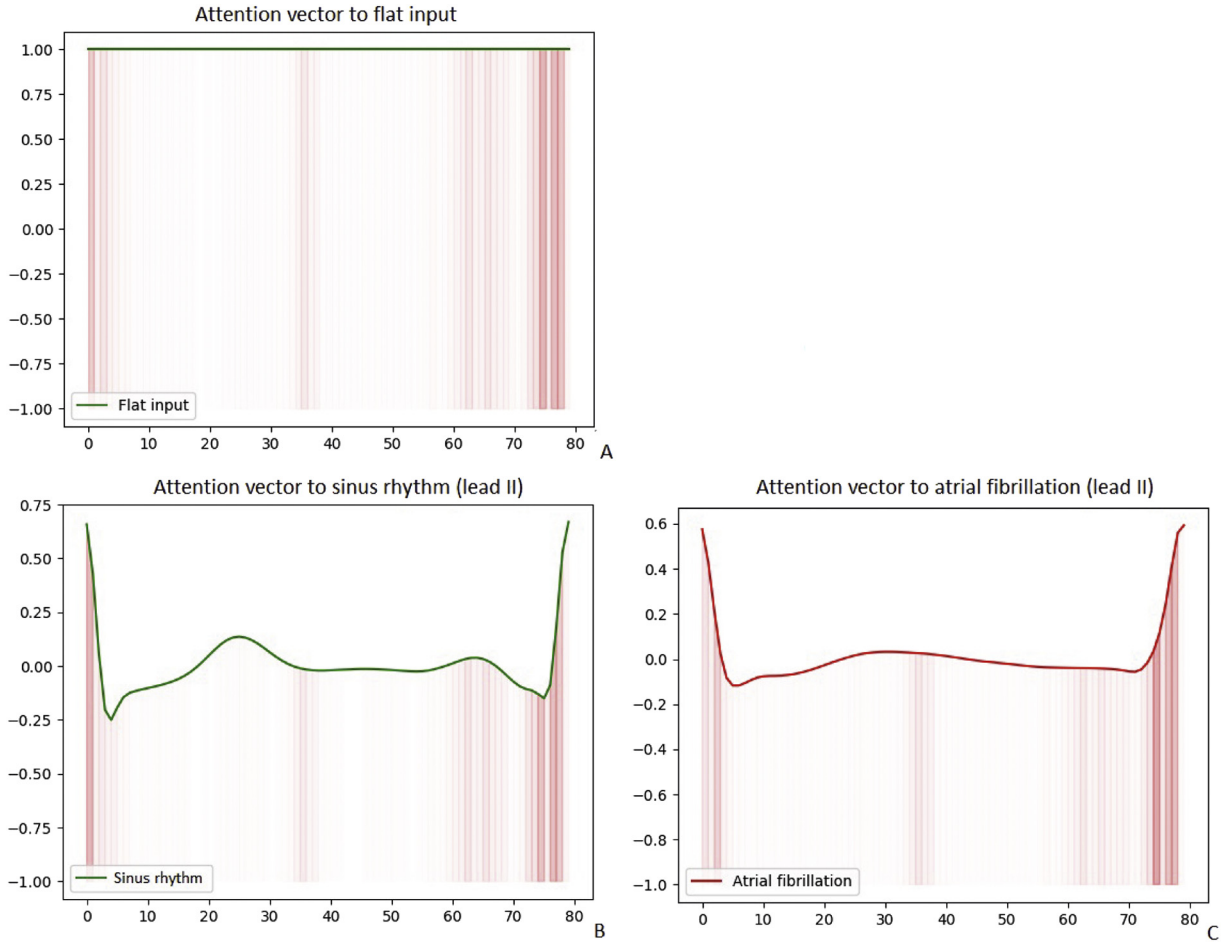

Fig. 3. Visualization of the attention vector of the different areas of the ECG for the DL model to discriminate AF from SR. (A) Demonstrates which data points the model is using to come to the correct classification after feeding the model a flat input. (B+C) Demonstrate the corresponding areas on a R-to-R wave SC-ECG sample in SR (B) or AF (C). The onset of the QRS complex proved to be the most relevant area for the model to discriminate AF from SR.

Nevertheless, our results confirm that DL models may have the potential to improve the diagnostic performance of AF detection algorithms integrated in ECG machines, pacemakers, implantable defibrillators and wearable cardiac monitors.

4.2. Comparison with previous AF detection models

Many improved AF detection algorithms have been developed to detect AF in an efficient manner over the last years. Most of the current device-integrated algorithms are based on atrial activity (e.g. absence of P-waves), ventricular activity (Lorenz plot analysis, and RR-interval variance) or a combination of these [20]. More recently, AF detection algorithms have been developed that are mainly artificial intelligence (AI) based, using DL or machine learning (approaches. However, most published AI models cannot yet provide practical perspectives for real-life implementation in cardiac devices, as a gold standard of the best architecture or approach is lacking. The PhysioNet/Computing in Cardiology (CinC) challenge in 2017 encouraged engineers to develop an algorithm to differentiate AF from noise or SR using short 12,186 single lead ECGs of 9–16 s recorded by AliveCor [21]. The 75 teams that participate in the challenge had the full play to use different methods to develop the best performing AF discrimination algorithm defined as the highest F1 score. Four teams won the challenge with an equal F1-score of 0.83, their methods varied from random forests to DL based algorithms [8,21]. Our best performing DL model although developed on a different and smaller dataset, reached a considerably higher F1 score of 0.94 (Table 1) than the reported winning models in the CinC challenge. The model presented in this paper did not outperform all currently reported AF detection or rhythm discrimination algorithms. Athif et al. report a similar performance of their morphology based AF detection model, with an accuracy of 0.96 [22]. However, Athif et al. used predefined statistical and morphology features as input for their model, in contrast to our methods wherein we did not dictate the computer what the most important features are to discriminate AF from SR. The capability of DL to choose features without human interference is what we think one of the most fascinating aspect of this approach. Indeed we show that -somewhat unexpectedly- the onset of the QRS complex is the most sensitive segment for AF discrimination. AF detection models that have been reported to perform slightly better than our model, are all using a DL based approach consisting of neural networks [4,23,24], and are associated with accuracies up to 99.7% [23]. Most of these studies used a form of pre-processing of the raw data to feed in to the DL model without losing important features of the signal. DL based rhythm discrimination studies using much larger datasets than in this study show the feasibility of using ECG data without the need of pre-processing and thus enabling a further automated end-to-end DL approach [6]. The promising results of DL technology based algorithms to detect AF allow to use this technology in other ways to detect or predict AF. Recently, Attia et al. showed that subtle patterns on ECG in SR could uncover the presence of a history

of AF in patients [25]. Besides that these encouraging results may improve clinical care and precision medicine for AF, finding ways to gaze into the black box of these models remains an area of ongoing investigation.

4.3. Deep learning model visualization

DL has the potential to integrate unrecognized features hidden in the raw data. This opens DL models to the critique that they consist of black boxes and that it is not revealed which elements of the data affect their predictions. To our best knowledge we are the first to open the black box of our AF detection algorithm in a way that shows clinicians in a simple manner which morphologic features of the ECG are the most important for the model to derive to the correct classification of AF or SR. We sought to elucidate how our DL model weighs each data point of the ECG complex by heat mapping the input signal of a single cardiac cycle. Our results demonstrate that the current R-to-R wave representation model focuses on the presence of the P-wave, the onset of the QRS complex and on early and late components of the T-wave. The fact that the earliest activation of the QRS complex is the most relevant area for the model could be explained in several ways. First, the early activation of the QRS complex includes the atrial repolarization, which is indiscernible on the ECG in AF, but may be affirmative picked up by the model in SR. Second, the existence of atrial fibrillatory waves in ECGs in AF, which may be more pronounced at the start of the QRS complex [26]. The model was not trained on wider QRS complexes as there was no difference in QRS duration between both groups (Table 1A, supplementary).

4.4. Clinical implications

Unrecognized or untreated AF is responsible for more than a third of all ischemic strokes [27]. The first step in the reduction of AF related strokes is timely detection of AF to initiate oral anticoagulation therapy in patients at risk for stroke. Current standard of care for the detection of AF is capturing an episode of AF on an ECG, Holter monitoring or detection by cardiac implantable electronic devices. However, the accuracy of most AF algorithms of these devices is low, and need human validation to confirm the diagnosis of AF. Integrating AI-based AF detection algorithms in ECG machines and devices may lead to an enormous improvement in accuracy of AF detection which may lead to improved AF detection, timely initiated therapy and thereby a reduction in health care expenditure.

Using SC-ECG samples, or ECG segments of a small duration is feasible and may be of great potential, in particular for wearable devices/sensors wherein long term duration recording storage is limited.

In our tertiary referral center, with a database with raw data of more than 1.5 million ECGs, our work may act as a pilot study for future AI based models for the improvement in the prediction, pathophysiology and management for AF that may lead to personalized therapy selection for AF. For example, an algorithm to predict AF in patients at high risk-but without a history of AF on ECGs in SR could be developed. Similarly, SC-samples as features in machine learning prediction models may be used for outcome prediction of several interventions for AF. In addition, our approach to use ECGs for AI models may serve as a tool to develop other AI based models for the electrocardiographic detection and prediction of disease. However, it must be said, as there an enormous ways to intergrade raw ECG data into DL model, that the use of SC-samples only may not be the holy grail of data input. Alternately, an end-to-end approach without the need of pre-processing may have the preference of choice.

4.5. Limitations

Our study has several limitations. First, we used an ECG dataset of just 240 patients diagnosed with AF where the rate of SR and AF ECGs were artificially balanced, instead of using a large unselected cohort with a low incidence of AF. Thereby, we excluded ECGs in atrial flutter; however also in these patients anticoagulation therapy is required. Additionally, we only used limited information from single cardiac cycles of one single lead in the current models separately. A future algorithm should include data from all available leads and incorporate R-R interval variation to further improve performance. We only used the Fourier Cosine Series in the baseline pre-processing steps of the development of the model. Using the Fourier Cosine Series as input for a neural network could further improve the training speed, reduce complexity of the model and improve accuracy. Last, we only applied our visualization method on a simplified architecture of the DL architecture with the best performance (accuracy: 0.88; ROC-AUC 0.93). The decreased performance of this approach may have affected the heat mapping results, and may not fully represent our best performing model. Future improvements in visualization techniques are needed to determine the attention vector of the more complex models, and will further guide us in visualizing and understanding current and future DL models.

5. Conclusion

We demonstrate that a morphology based DL model using SC-ECG samples discriminate AF from SR with a very high accuracy. The most relevant ECG segment for the discrimination between AF and SR is the onset of the QRS complex. DL model visualization tools may help clinicians gain insight into unrecognized ECG features for AF or more complex electrocardiography.

Supplementary data to this article can be found online at https://doi.org/10.1016/j.ijcard.2020.04.046.

CRediT authorship contribution statement

Sarah W.E. Baalman: Conceptualization, Methodology, Writing - original draft, Resources, Visualization, Project administration. **Florian E. Schroevers:** Methodology, Software, Visualization, Writing - original draft. **Abel J. Oakley:** Methodology, Software, Visualization, Writing - original draft. **Tom F. Brouwer:** Conceptualization, Writing - review & editing. **Willeke van der Stuijt:** Writing - review & editing. **Hidde Bleijendaal:** Writing - review & editing. **Lucas A. Ramos:** Software, Writing - review & editing. **Ricardo R. Lopes:** Software, Writing - review & editing. **Henk A. Marquering:** Software, Writing - review & editing. **Reinoud E. Knops:** Resources, Supervision, Writing - review & editing. **Joris R. de Groot:** Resources, Data curation, Supervision, Funding acquisition, Writing - review & editing.

Declaration of competing interest

Baalman, Schroevers, Oakley, Van der Stuijt, Ramos, Lopes, Bleijendaal and Marquering report no relationships that could be constructed as conflicts of interest. Brouwer reports compensation for services from Boston Scientific. Knops reports consulting fees, research grants and honoraria for Boston Scientific, consulting fees research grants with Medtronic and Abbott. De Groot reports research grants from the Dutch Organization for Scientific Research, Abbott, AtriCure, Boston Scientific, Medtronic, consulting fees for Articure, Bayer, Diachii Sankyo, J&J, Novartis and Sewie.

References

[1] P. Kirchhof, S. Benussi, D. Kotecha, et al., 2016 ESC Guidelines for the management of atrial fibrillation developed in collaboration with EACTS, Eur. Heart J. 37 (38) (2016) 2893–2962.
[2] A.P. Shah, S.A. Rubin, Errors in the computerized electrocardiogram interpretation of cardiac rhythm, J. Electrocardiol. 40 (5) (2007) 385–390.
[3] Comparative study of algorithms for atrial fibrillation detection, in: N. Larburu, T. Lopetegi, I. Romero (Eds.),2011 Computing in Cardiology, 2011 , 18–21 Sept. 2011.

[4] R.S. Andersen, A. Peimankar, S. Puthusserypady, A deep learning approach for real-time detection of atrial fibrillation, Expert Syst. Appl. 115 (2019) 465–473.
[5] A deep learning approach to monitoring and detecting atrial fibrillation using wearable technology, in: S.P. Shashikumar, A.J. Shah, Q. Li, G.D. Clifford, S. Nemati (Eds.),2017 IEEE EMBS International Conference on Biomedical & Health Informatics (BHI), 2017 , 16–19 Feb. 2017.
[6] A.Y. Hannun, P. Rajpurkar, M. Haghpanahi, et al., Cardiologist-level arrhythmia detection and classification in ambulatory electrocardiograms using a deep neural network, Nat. Med. 25 (1) (2019) 65–69.
[7] Y. LeCun, Y. Bengio, G. Hinton, Deep learning, Nature 521 (2015) 436.
[8] R. Kamaleswaran, R. Mahajan, O. Akbilgic, A robust deep convolutional neural network for the classification of abnormal cardiac rhythm using single lead electrocardiograms of variable length, Physiol. Meas. 39 (3) (2018), 035006. .
[9] O. Faust, Y. Hagiwara, T.J. Hong, O.S. Lih, U.R. Acharya, Deep learning for healthcare applications based on physiological signals: a review, Comput. Methods Prog. Biomed. 161 (2018) 1–13.
[10] C. Krittanawong, K.W. Johnson, R.S. Rosenson, et al., Deep learning for cardiovascular medicine: a practical primer, Eur. Heart J. 40 (25) (2019) 2058–2073.
[11] A.H.G. Driessen, W.R. Berger, S.P.J. Krul, et al., Ganglion plexus ablation in advanced atrial fibrillation: the AFACT study, J. Am. Coll. Cardiol. 68 (11) (2016) 1155–1165.
[12] A. Savitzky, M.J.E. Golay, Smoothing and differentiation of data by simplified least squares procedures, Anal. Chem. 36 (8) (1964) 1627–1639.
[13] H.S. Carslaw, Introduction to the Theory of Fourier's Series and Integrals, Macmillan and Company, Limited, 1921.
[14] P. Hamilton, Editor open source ECG analysis, Comput. Cardiol. 2002 (Sept. 2002) 22–25.
[15] M. Sokolova, N. Japkowicz, S. Szpakowicz, Beyond accuracy, f-score and ROC: a family of discriminant measures for performance evaluation, Proceedings of the 19th Australian Joint Conference on Artificial Intelligence: Advances in Artificial Intelligence; Hobart, Australia. 2173281, Springer-Verlag 2006, pp. 1015–1021.
[16] S. Carter, C. Olah, Attention and augmented recurrent neural networks, Distill (2016) 1–16, https://doi.org/10.23915/distill.00001.
[17] GitHub Enterprise, , Available from https://github.com/enterprise.
[18] M.H. van der Ree, R.A. Scholte, P.G. Postema, J.R. de Groot, Playing by the rules: impact of the new General Data Protection Regulation on retrospective studies: a researcher's experience, Eur. Heart J. 40 (24) (2019) 1900–1902.
[19] D.P. Kingma, J. Ba, Adam: A Method for Stochastic Optimization, ICLR, 2015.
[20] H. Khamis, J. Chen, J. Stephen Redmond, N.H. Lovell, Detection of atrial fibrillation from RR intervals and PQRST morphology using a neural network ensemble, Conf Proc IEEE Eng Med Biol Soc. 2018 2018, pp. 5998–6001.
[21] G.D. Clifford, C. Liu, B. Moody, et al., AF classification from a short single lead ECG recording: the PhysioNet/Computing in Cardiology Challenge 2017, Comput Cardiol 2017 (44) (2010)https://doi.org/10.22489/CinC.2017.065-469.
[22] M. Athif, P.C. Yasawardene, C. Daluwatte, Detecting atrial fibrillation from short single lead ECGs using statistical and morphological features, Physiol. Meas. 39 (6) (2018), 064002. .
[23] O. Faust, A. Shenfield, M. Kareem, et al., Automated detection of atrial fibrillation using long short-term memory network with RR interval signals, Comput. Biol. Med. 102 (2018) 327–335.
[24] X. Fan, Q. Yao, Y. Cai, et al., Multiscaled fusion of deep convolutional neural networks for screening atrial fibrillation from single lead short ECG recordings, IEEE J. Biomed. Health Inform. 22 (6) (2018) 1744–1753.
[25] Z.I. Attia, P.A. Noseworthy, F. Lopez-Jimenez, et al., An artificial intelligence-enabled ECG algorithm for the identification of patients with atrial fibrillation during sinus rhythm: a retrospective analysis of outcome prediction, Lancet. 394 (10201) (2019) 861–867.
[26] M. Henriksson, A. García-Alberola, L. Sörnmo, Short-term reproducibility of parameters characterizing atrial fibrillatory waves, Comput. Biol. Med. 117 (2020) 103613.
[27] B. Freedman, T.S. Potpara, G.Y. Lip, Stroke prevention in atrial fibrillation, Lancet. 388 (10046) (2016) 806–817.